

Tunable Dispersion Compensators Utilizing Higher Order Mode Fibers

S. Ramachandran, S. Ghalmi, S. Chandrasekhar, *Fellow, IEEE*, I. Ryazansky, M. F. Yan, F. V. Dimarcello, W. A. Reed, and P. Wisk

Abstract—We demonstrate a novel tunable dispersion compensator that utilizes higher order mode fibers and switchable fiber gratings. The device is broad band and wavelength continuous, yielding a bit rate, bit format, and signal bandwidth as well as channel-spacing transparent adjustable dispersion compensator. The novel device design is free from tradeoffs between tuning range and bandwidth. The tuning range is 435 ps/nm, with a bandwidth of 30 nm. Its all-fiber configuration yields the lowest loss (average ~ 3.7 dB) tunable dispersion compensator reported to date. 40-Gb/s transmission tests reveal penalty-free operation.

Index Terms—Gratings, optical communication, optical components, optical delay lines, optical fiber devices, optical fiber dispersion.

I. INTRODUCTION

LONG-HAUL high-speed transmission links are designed with tight tolerances on their dispersion maps. Statistical variations in the dispersion of transmission fibers, amplifier-hut spacings, or ambient conditions can lead to significant transmission penalties. One way to address this problem is by introducing tunable dispersion compensators (TDCs) that can provide either dynamic or set-able control. Dynamic control is needed to offset dispersion variations due to environmental changes. Alternatively, set-able dispersion control can address variations in network link design arising from manufacturing variations in transmission fiber spans or the distance between amplifier huts. A broad-band means for set-able dispersion control also facilitates link design by allowing the prospect of “mixing and matching” different fiber types to realize a transmission span.

TDCs reported to date exploit the frequency-dependent phase response of an optical filter. Examples include planar waveguide-based devices such as ring resonators [1] and waveguide gratings [2], free-space devices such as tunable etalons [3] and virtually imaged phase arrays [4], and chirped fiber Bragg gratings [5],[6]. The bandwidth of these devices is limited because they can function only in a restricted passband within the bandwidth of the filter. Thus, such filters must be specifically designed for particular signal bandwidths, which in turn depend on the bit rates as well as bit formats. These devices may be tailored to operate on several channels of an optical link by making

the filter response spectrally periodic. However, this requires *a priori* knowledge of the channel spacing. For the above reasons, while existing TDCs offer an attractive means to manage dispersion variations in an optical link, they do not possess the versatility, bandwidth, and low-loss characteristics of their widely deployed static counterpart, namely, dispersion compensating fibers (DCFs).

In this letter, we demonstrate the first wavelength-continuous broad-band adjustable dispersion compensator. The significant distinction from other TDCs is that it is simultaneously broad band, wavelength continuous, and low loss. This implies that the device is transparent to bit rates, bit formats, and channel spacings. Thus, they combine the advantages of tunability available from other TDCs, with the universally transparent characteristics of static DCFs. Furthermore, there are no inherent tradeoffs between tuning range and bandwidth, as is the case for other TDCs. This enables the prospect of deploying TDCs in-line in a transmission link, as well as at the receiver.

The device exploits optical path diversity afforded by routing light in either the LP_{01} or LP_{02} mode of a higher order mode (HOM) fiber. The routing is achieved by a series of 2×2 switches that shuffle light between the LP_{01} and LP_{02} modes in the HOM fiber. The dispersive feature is fiber-waveguide dispersion, as with (static) HOM dispersion compensators (HOM-DC) [7] and DCFs. Hence, this device retains all the advantages of HOM-DCs: low nonlinearities, slope-matching ability, large bandwidth (30 nm), low multipath interference ($MPI < -39$ dB), and low loss (average ~ 3.7 dB), while providing tunable dispersion. The adjustable HOM (AHOM) device demonstrated here has a tuning range of 435 ps/nm, and can be tuned over the entire range in discrete, equally spaced steps of 14 ps/nm.

Transmission tests conducted with 40-Gb/s carrier-suppressed return-to-zero (CSRZ) signals reveal penalty-free operation over the entire dispersion tuning range. Bit-error-rate (BER) measurements were conducted at several wavelengths across the C-band to confirm the broad-band nature of the AHOM.

II. DEVICE SCHEMATIC AND CHARACTERISTICS

The schematic of the AHOM is shown in Fig. 1(a). It illustrates that the device comprises five segments of HOM fiber arranged in a binary length progression, with 2×2 mode-converting switches, comprising switchable long-period fiber gratings (SLPGs) between each segment. The HOM fibers support the LP_{01} and LP_{02} modes, with dispersion values of +21 and

Manuscript received November 4, 2002; revised December 19, 2002.

S. Ramachandran, S. Ghalmi, I. Ryazansky, M. F. Yan, F. V. Dimarcello, W. A. Reed, and P. Wisk are with OFS Laboratories, Murray Hill, NJ 07974 USA (e-mail: sidr@ofsophics.com).

S. Chandrasekhar is with Bell Laboratories, Lucent Technologies, Holmdel, NJ 07733 USA.

Digital Object Identifier 10.1109/LPT.2003.810255

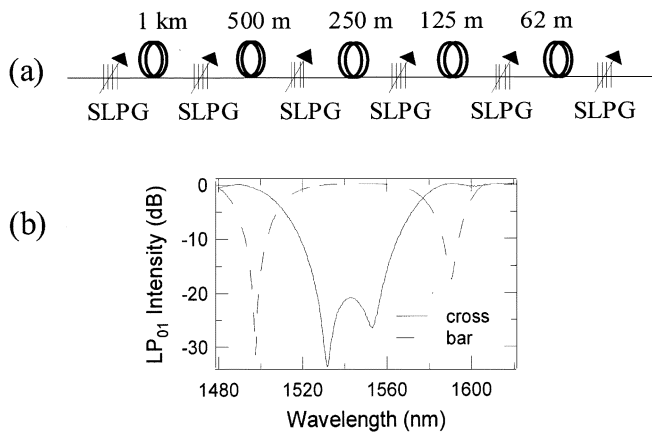


Fig. 1. (a) AHOM schematic—binary length progression of HOM fibers with SLPGs as 2×2 switches. (b) Spectrum of SLPG in the cross and bar states—broad band in both states.

$-203 \text{ ps/nm} \cdot \text{km}$ at 1550 nm , respectively. The SLPGs determine the mode in which the signal propagates in the HOM fiber. Thus, the device dispersion is determined by the state of the SLPG switches, which in turn determine the relative lengths of fiber over which the signal propagates in either the LP_{01} and LP_{02} modes, respectively. The upper and lower limits of dispersion are attained when the signal travels exclusively in one of the two modes. Since two optical paths exist in each segment, $2^5 = 32$ distinct optical paths, or 32 distinct dispersion values are achievable with the five-segment device shown in Fig. 1(a).

The building block for the 2×2 switches are LPGs induced in specially designed HOM fibers. LPGs induced in HOM fibers have previously been demonstrated to yield strong (20 dB) mode conversion over bandwidths exceeding 60 nm [8]. A unique feature of these LPGs is that their mode conversion strength changes when they are temperature or strain tuned. This feature is used to realize mode-converting switches. LPGs with lengths of 3 cm are written in HOM fibers, and packaged in stainless steel tubes that can be heated with resistive wires. Fig. 1(b) shows the spectrum of such an SLPG in the “cross” state (mode-converting state) and “bar” state (no mode conversion), respectively. As is evident, mode conversion greater than 20 dB is achieved over a 30-nm bandwidth from 1528 to 1558 nm. Switching times were approximately 2 min for this device, owing to the design of the current tuning package that comprises bulk components. The speed may be significantly increased by implementing alternate tuning mechanisms, such as resistive thin-film heaters that can provide 100-ms time-scale switching.

Fig. 2 shows dispersion measurements for a variety of AHOM switch states. As shown in Fig. 1(a), this device comprises five segments of HOM fibers arranged in a binary length progression. It can be shown that binary length progressions ensure equally spaced dispersion step sizes. Thus, the length of the smallest HOM fiber segment (62 m, for this device) dictates the step size (14 ps/nm). As is evident from Fig. 2, there are several unique features of this TDC. The dispersion tuning range and step size can be arbitrarily varied, since they depend only on the total fiber length, and the length of the smallest segment, respectively. The bandwidth of the device is independently set

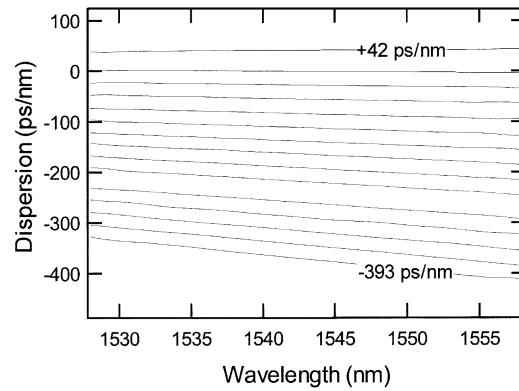


Fig. 2. Dispersion versus wavelength. Tuning range = 435 ps/nm in 14-ps/nm steps at 1550 nm (only 30-ps/nm steps shown in plot for clarity). Wavelength-continuous response over 30 nm.

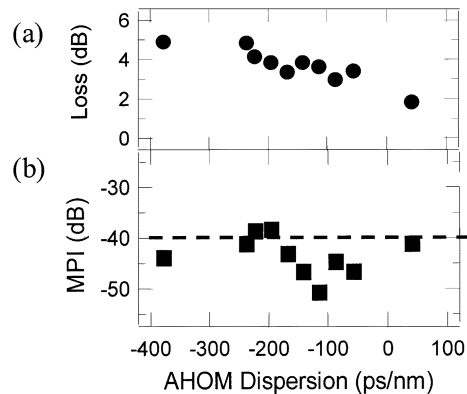


Fig. 3. (a) AHOM insertion loss versus dispersion for different states. Average loss $\sim 3.7 \text{ dB}$, max $\sim 5 \text{ dB}$. (b) MPI versus dispersion. $\text{MPI} < -39 \text{ dB}$ for all states, average MPI $\sim -44 \text{ dB}$.

by the length of the grating. While the current device has 30-nm bandwidth, similar mode-conversion gratings with 63-nm bandwidths have been demonstrated, indicating that the AHOM can potentially cover the entire C - or L -band. Most significantly, the spectral response is wavelength continuous, since the dispersion is due to the fiber itself. This implies that the device can operate at any bit rate, bit format, and channel spacing.

Fig. 3(a) shows the insertion loss of the device at 1545 nm , for various switch states spanning the tuning range. The average loss is 3.7 dB , which is the lowest value reported for any broad-band TDC. However, loss excursions of 3 dB (between various switch states) were observed. A loss analysis of this device was conducted by a cutback process in which several AHOMs with varying numbers of segments were constructed. The loss contribution due to each additional mode converter was below the measurement limit of 0.1 dB , demonstrating that the HOM fiber-based SLPGs are the lowest loss 2×2 switches reported to date. On the other hand, splice losses between identical HOM fibers were found to be as high as 0.3 dB/splice for the LP_{02} mode. Since a device with six SLPGs contains 12 splices, a majority of the device loss is attributed to splice loss. This implies that an AHOM with significantly lower loss is feasible since splices between similar fibers can be optimized to yield negligible loss.

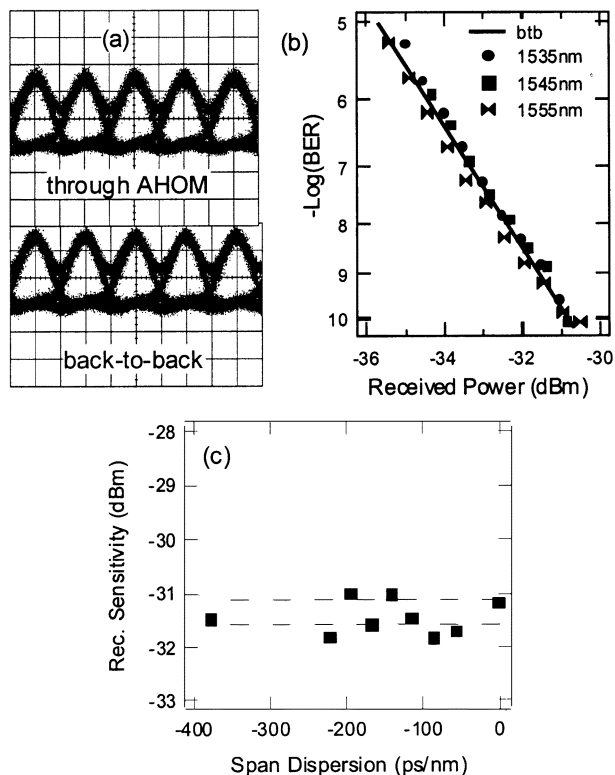


Fig. 4. Dispersion versus wavelength. Tuning range = 435 ps/nm in 14 ps/nm steps at 1550 nm (only 30 ps/nm steps shown in plot for clarity). Wavelength-continuous response over 30 nm. RDS varies between 0.003 and 0.0074 nm.

The existence of multiple splices and mode converters has the potential to cause signal distortions due to multipath interference (MPI). The MPI of the AHOM was deduced by measuring temporal intensity fluctuations over 500 ms, of 1545-nm continuous-wave light from a DFB laser sent through the module. The measured MPI [Fig. 3(b)] is less than -39 dB for all measured AHOM switch states. In fact, it is significantly lower (MPI ~ -44 dB, on the average) for the majority of states measured. This represents a negligible level of signal distortion, since an average MPI ~ -44 dB implies that more than 50 such devices concatenated in series will yield less than 1-dB BER power penalties.

The MPI measurements were conducted *after* the tuning action is completed. One issue of concern is that the AHOM in its present configuration is blocking while being tuned. However, this is not a limitation for a set-able device. In addition, it is conceivable that dynamic tuning can be achieved by AHOMs with significantly faster switching times or alternate switching configurations.

III. TRANSMISSION PERFORMANCE

Systems evaluations of the AHOM were carried out with 40-Gb/s CSRZ (67% duty cycle) signals in the *C*-band. First, the AHOM was tested in the switch state that yielded the highest dispersion, since it is the state that exhibits the highest loss, and may be most susceptible to MPI distortions. CSRZ signals were transmitted through a span comprising TWRS and TW-Reach fibers (span dispersion $\sim +377$ ps/nm at 1545 nm). The AHOM switch state was adjusted to yield -378 ps/nm at

1545 nm. The open eye in Fig. 4(a) qualitatively confirms the low MPI, dispersion-compensating capability of the AHOM. To quantify this, BER measurements were conducted for the same span at 1535, 1545, and 1555 nm, respectively. Fig. 4(b) shows that the BER curves at all three wavelengths essentially overlap with the back-to-back measurement, indicating that the AHOM is broad band, and induces no distortions due to MPI. No additional tuning of the AHOM was required when measuring the BER at the three different wavelengths, indicating that the AHOM provided adequate dispersion slope as well as dispersion compensation for the span.

The dispersion-tuning characteristic of the AHOM was tested by measuring receiver sensitivities at a BER of 10^{-9} for 40-Gb/s 1545-nm signals. Several different transmission fiber spans (comprising combinations of TWRS and TW-Reach fibers) with different lengths were assembled, and the AHOM was tuned to the appropriate values to yield the closest match in dispersion. Fig. 4(c) shows the receiver sensitivity for the different spans (with different dispersion values) compensated by the AHOM tuned to the corresponding optimal state. The two horizontal dashed lines show back-to-back receiver sensitivities from two separate measurements, indicating 0.4-dB measurement uncertainty. As is evident from Fig. 4(c), penalty-free transmission (within the measurement error) is achieved for AHOM states spanning its entire tuning range.

IV. SUMMARY

We have demonstrated the first wavelength-continuous broad-band adjustable dispersion compensator. The device possesses no inherent bandwidth versus tunability tradeoffs. It is the first adjustable compensator that is bit-rate bit-format wavelength as well as channel spacing transparent, opening the prospect of in-line deployment of TDCs. Systems evaluations reveal penalty-free transmission at 40 Gb/s with the AHOM.

REFERENCES

- [1] C. K. Madsen, "Integrated waveguide allpass filter tunable dispersion compensators," in *Proc. OFC*, 2002, Paper TuT-1.
- [2] C. R. Doerr, L. W. Stultz, S. Chandrasekhar, L. Buhl, and R. Pafchek, "Multichannel integrated tunable dispersion compensator employing thermo-optic lens," in *Proc. OFC*, 2002, Paper FA6.
- [3] L. M. Lunardi, D. J. Moss, S. Chandrasekhar, and L. L. Buhl, "An etalon-based tunable dispersion compensator (TDC) device for 40-gbit/s applications," in *Proc. ECOC*, 2002, Paper 5.4.6.
- [4] M. Shirasaki and S. Cao, "Compensation of chromatic dispersion and dispersion slope using a virtually imaged phased array," in *Proc. OFC*, 2001, Paper TuS-1.
- [5] B. J. Eggleton, A. Ahuja, P. S. Westbrook, J. A. Rogers, P. Kuo, T. N. Nielsen, and B. Mikkelsen, "Integrated tunable fiber gratings for dispersion management in high-bit rate systems," *J. Lightwave Technol.*, vol. 18, pp. 1419–1432, Oct. 2000.
- [6] X.-J. Cai, K.-M. Feng, A. E. Willner, V. Grubsky, D. S. Starodubov, and J. Feinberg, "Simultaneous tunable dispersion compensation of many WDM channels using a sampled nonlinearly chirped fiber Bragg grating," *IEEE Photon. Technol. Lett.*, vol. 11, pp. 1455–1457, Nov. 1999.
- [7] S. Ramachandran, B. Mikkelsen, L. C. Cowsar, M. F. Yan, G. Raybon, L. Boivin, M. Fishteyn, W. A. Reed, P. Wisk, D. Brownlow, R. G. Huff, and L. Gruner-Nielsen, "All-fiber, grating-based, higher order mode dispersion compensator for broad-band compensation and 1000-km transmission at 40 Gb/s," *IEEE Photon. Technol. Lett.*, vol. 13, pp. 632–634, June 2001.
- [8] S. Ramachandran, Z. Wang, and M. F. Yan, "Bandwidth control of long-period grating-based mode converters in few-mode fibers," *Opt. Lett.*, vol. 27, p. 698, 2002.